Oligothiophene Catenanes and Knots: A Theoretical Study

Serguei Fomine* and Patricia Guadarrama

Instituto de Investigaciones en Materiales, Universidad Nacional Autónoma de México, Apartado Postal 70-360, CU, Coyoacán, México DF 04510, México

Received: May 18, 2006; In Final Form: June 30, 2006

Oligothiophene [2]catenanes and knots containing up to 28 thiophene units have been studied at the BHandHLYP/3-21G* level of theory. Small knots (less than 22 thiophene units) and [2]catenanes (less than 18 thiophene units) are strained molecules. Larger knots and [2]catenanes are almost strain-free. [2]Catenanes and knots having less than 18 and 24 units, respectively, show transversal electronic coupling destroying one-dimensionality of molecules reflecting in smaller band gaps compared to larger knots and catenanes. Ionization potentials of knots and catenanes are always higher compared to that of lineal oligomers due to less effective conjugation. Polaron formation in catenanes is delocalized only over one ring, leaving another intact. In the case of a knot containing 22 thiophene units, estimated polaron delocalization is 8 to 9 repeating units.

Introduction

Recently, much attention has been paid to conjugated polymers having nonconventional architecture, such as hyperbranched, star-shaped, and cyclic, among others.[1] The use of nonconventional geometry allows one to tune electronic and other physical properties of conjugated polymers; moreover, exotic polymer architectures are excellent models to obtain deeper insight into the nature of electronic properties of the conjugated systems. Thus, it has been observed that supramolecular assemblies of regioregular polyalkylthiophenes have a two-dimensional well-organized lamellar structure[2] with reduced interchain separation (3.7−3.8 Å, thiophene ring stacking), and thus the mobility of positive carriers increases with respect to typical values.[3] Hence, both electronic and photophysical properties are significantly modified. The absorption spectrum is red-shifted, indicating an increase in the average conjugation length. These polymers exhibit smaller band gaps, better ordering, and crystallinity in their solid states, with improved electroconductivities.

Among conjugated polymers, polythiophenes are one of the most promising and investigated conjugated systems due to their synthetic availability, stability in various redox states, processability, and tunable electronic properties.[4] As a result, these are promising candidates for molecular electronic devices.[5−7]

Cyclic oligothiophenes having *n*-butyl units in positions 3 and 4[8] and cyclic oligopyrroles[9] have recently been prepared. A few articles were published describing these novel molecules and exploring their physical properties.[10] In a very recent article, cyclic oligothiophenes from $n = 6$ to 30 where n is the number of thiophene units were studied at the B3LYP/6-31G* level, revealing that cyclic polythiophene is an excellent model for linear polythiophenes.[11]

In the context of nanotechnology and, in general, in engineering science, the structures with controllable complexity might result in unexpected and probably more efficient responses. Thus, the access to a diversity of topologies may possibly benefit from the technological perspective. Knots and catenanes represent the next level topological complexity compared to simple annular topology.

In chemical topology,[12] the object is a molecule or a molecular assembly that is schematically represented on paper as a graph. If the graph contains crossings, then the graph and the molecule are referred to as nonplanar and topologically nontrivial, respectively. Figure 1 shows examples of both nonplanar (**I** and **II**) and planar (**III**) graphs. They are simplified projections of the enantiomers of the trefoil knot and a cycle, respectively. In [2]catenanes (**IV**), which represents a simplest link, two cyclic molecules are mechanically linked with each other. The disruption of a catenane into its separate components requires the breaking of one or more covalent bonds in the mechanically linked molecule. Thus, catenanes behave as well-defined molecular compounds with properties significantly different from those of their individual components.

This article describes a theoretical study of polythiophene knots and catenanes. Although a number of molecular knots and catenanes have been prepared to date,[13] no reports exist on preparation of totally conjugated knots or catenanes. This article is the first attempt to predict the most important properties of oligothiophene knots and catenanes using quantum chemistry tools and to compare them with cyclic and linear analogues.

Computational Details

The selection of a theoretical model is of primary importance for the correct prediction of the properties of unknown molecules. The choice of a theoretical model was based on its ability to reproduce geometry and band gaps of well-characterized oligothiophenes and the high-level calculation of binding energy in thiophene dimer which is important for taking into account long-range interactions between thiophene fragments in knots and catenanes. Among many tested theoretical models, the BHandHLYP hybrid functional in combination with the 3-21G* basis set as defined in Gaussian 03 package[18] was found to be the best compromise between computational efficiency and precision. Figure 2 shows calculated and experimentally determined bond lengths and angles for the central ring of thiophene hexamer (**T6**).[14]

* Corresponding author. E-mail: fomine@servidor.unam.mx.

10.1021/jp063065i CCC: $33.50
Published on Web 08/01/2006

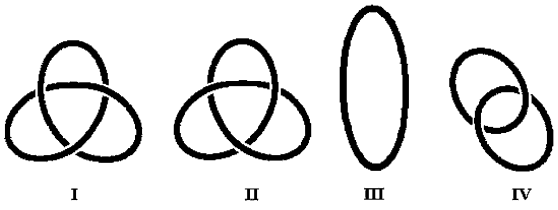

Figure 1. Simplified projections of the enantiomers of the trefoil knot (**I**, **II**), a cycle (**III**), and a [2]catenane (**IV**).

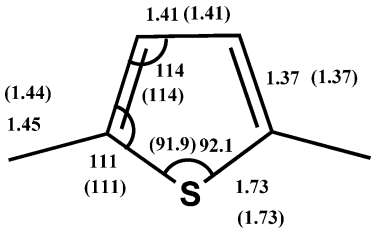

Figure 2. Calculated and experimentally determined (in parentheses) bond lengths for the central ring of thiophene hexamer (**T6**).[14]

TABLE 1: Binding Energies of Thiophene T-Shape Dimer at Different Levels of Theory (kcal/mol)

CCSD(T)/6-31G*// MP2/6-31G*	CCSD(T)/6-31g*// BHandHLYP/3-21g*	B97-1/3-21G*// BHandHLYP/3-21g*
−3.41	−3.36	−3.47

As seen, the BHandHLYP/3-21G* model shows excellent agreement with experiment. This model was used for all geometry optimizations. For band-gap calculations, the ZINDO/S model[15] was used with 10 virtual and 10 highest occupied molecular orbitals participating in CI. ZINDO/S was shown to be remarkably precise for the band-gap prediction in conjugated molecules.[16]

To estimate the intermolecular interactions between oligothiophene fragments in catenanes and knots, the model system calculations (thiophene dimer) were carried out. Due to the size of molecules under the study post HF methods were inapplicable. On the other hand, DFT methods were not reliable enough to treat weak interactions.

We focused on reproducing high-level binding energies for thiophene dimer using DFT. As seen from Table 1, the B97-1 functional[17] (B97-1/3-21G*//BHandHLYP/3-21g* model) reproduces very well CCSD(T)/6-31G*//MP2/6-31G* binding energies of thiophene dimer. The quality of geometry optimization of the dimer can be estimated comparing CCSD(T)/6-31G* binding energies obtained using geometries optimized at different theoretical levels. As seen, MP2/6-31G* and BHandHLYP/3-21G* optimized geometries give quite similar CCSD(T)/6-31G* binding energies.

[2]-Catenanes and trefoil knots consisting of up to 28 thiophene units have been studied. For comparison purpose, lineal oligomers up to 28 and cyclic structures up to 14 thiophene units have been calculated as well. Linear and cyclic oligomers are denoted as **Tn** and **Cn**, respectively, where **n** is the number of thiophene units. [2]Catenanes and trefoil knots are denoted as **CATn** and **KNOTn**. First, successive conformational searches have been carried out using mixed torsional/large-scale low-mode sampling algorithm incorporated in the Macromodel 9.0 suite of programs using OPLS-AA force field in the gas phase. Each conformational search included 10 000 iterations. Obtained lowest-energy structures were then used in DFT optimizations without any symmetry restrictions. For cyclic

SCHEME 1: Isodesmic Reaction Used for Calculation of Strain Energies

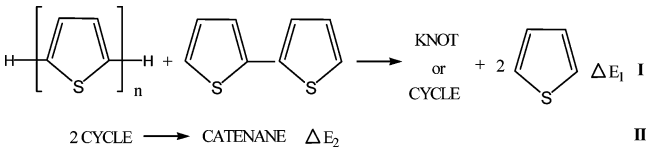

structures (from **C7** to **C14**), the lowest-energy structures located by conformational search were all syn conformers, which is in line with ref 11, where all syn and all anti cyclic conformers were optimized at the B3LYP/6-31G* level. Neutral molecules were calculated using restricted closed-shell Hartree−Fock formalism; cation radicals were treated at the restricted open shell level. All calculations were performed using the Gaussian 03 program.[18] To calculate strain energy, an isodesmic reaction shown in Scheme 1 was used. The strain energy (E_s) of cycles and knots is ΔE_1, while the strain energy of catenanes was estimated as $2\Delta E_1 + \Delta E_2$, where ΔE_1 and ΔE_2 are the corresponding reaction energy calculated at the B97-1/3-21G*// BHandHLYP/3-21G* level of theory.

Results and Discussion

Geometry and Strain Energy of Neutral Molecules. Figures 3 and 4 show optimized structures of knots and catenanes, respectively. In the lowest-energy conformers of knots, a mixture of syn- and anti-oriented thiophene rings exists except for **KNOT22** where all rings have syn orientation. For large knots, **KNOT24** and **KNOT28** oligothiophene fragments that are almost linear have anti orientation while more curled fragments contain syn-oriented rings. This agrees with the fact that for linear polyphiophene anti conformation is the most stable, while for cyclic oligothiophenes containing from 8 to 20 units the most stable conformation is all syn.[11] Large catenanes (from **CAT18** to **CAT28**) have all syn conformation of thiophene units. They are made of two cyclic oligothiohenes and are strain-free. (Figure 5). As a consequence, cycles maintain relative orientation of thiophene rings in large catenanes. For small catenanes (**CAT14** and **CAT16**), there are sequences of syn- and anti-oriented thiophene rings.

Table 2 shows calculated bond lengths in knots and catenanes. For comparison, the bond lengths in cyclic and linear molecules are also listed. If we take the bond lengths in **T28** (central ring) as a reference, one can see that small catenanes and especially knots are extremely strained.

Thus, for **KNOT16** the inter-ring bond length increases to 1.485 Å compared to 1.437 Å for **T28**. For **CAT16** the elongation is less but still significant (1.466 Å). The less-affected bond is $C_2{=}C_3$. In large knots and catenanes, the bond lengths are similar to those of linear oligothiophenes. Thus, starting from **CAT18** and **KNOT22** the difference does not exceeds 0.02 Å. Figure 5 shows strain energies calculated for knots, catenanes, and cyclic molecules. As seen, knots are more strained compared to corresponding catenanes. However, for knots the strain energy decreases more rapidly with the number of thiophene units compared to catenanes. As a result, the difference in strain energy between **CAT28** and **KNOT28** almost disappears, while for **CAT16** and **KNOT16** this difference reaches 218.4 kcal/mol. Considering studied molecules as synthetic targets, one must look at the strain energy per repeating unit. Catenanes starting from **CAT22** may be considered practically strain-free with strain energy per unit less than 1 kcal/mol. **KNOT24** and **KNOT28** also have very low strain energy, close to that of **C12**, the substituted analogue of which has recently been synthe-

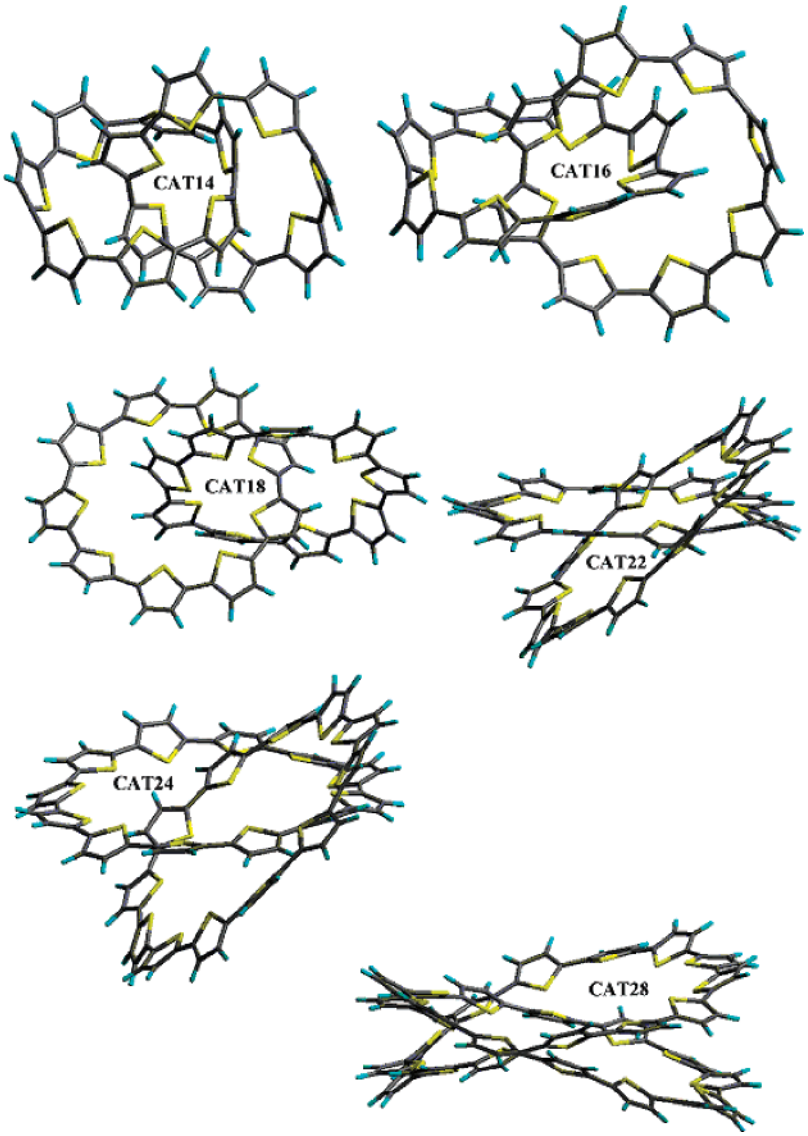

Figure 3. BHandHLYP optimized structures of catenanes.

sized.[19] One can compare calculated strain energies for **C8**, **C12**, and **C14** with that calculated by Sanjio and Bendikov[11] using a different technique at the B3LYP/6-31G* level of theory (45, 12, and 14 kcal/mol), which qualitatively agrees with our estimation (39.4, 9.4, 9.5 kcal/mol). The method adopted in this study for the calculation of strain energy gives strain energy of 32 kcal/mol for cyclobutene, close to the experimental value (30 kcal/mol).[20]

Since the catenane molecule contains two oligothiophene cycles, the interactions between them can be estimated as a difference of total electronic energy of a catenane and a sum of total electronic energies of corresponding cycles. As seen from Figure 5, the binding energies of small catenanes are positive due to steric hindrances between two rings representing a significant part of total strain energy. Thus, for **CAT14**, interring interaction represents 24.9 out of a total 142.5 kcal/mol strain energy. For larger catenanes starting from **CAT18** the binding energy becomes negative, reaching −17.2 kcal/mol for **CAT28** due to $\pi-\pi$ stacking. This binding between oligothiophene rings could be used for the template synthesis of thiophene-containing catenanes. It is seen from Figure 3 that an increase in binging between cycles is reflected in conformational changes of catenanes. In **CAT14**, **CAT16**, and **CAT18**, oligothiophene cycles are perpendicular to each other, while for **CAT22**, **CAT24**, and **CAT28** the dihedral angle between cycles continuously decreases due to interactions.

Band Gaps of Neutral Molecules. Table 3 shows calculated band gaps for linear, cyclic oligothiophenes, knots, and catenanes. As seen, the ZINDO/S model reproduces well available experimental band gaps for linear oligothiophenes, giving the band gap of 2.21 eV for **T28**. This value is close to 2.2 eV, which is the experimentally determined band gap for polythiophene. It is reported that the absorption maxima for the macrocyclic cyclothiophenes are found at approximately the energies at which linear compounds with half the number of repeating units absorb.[10a] Our calculations agree with this observation. As seen from Table 3, oligomers **T4**, **T6**, **T7**, **C8**, **C12**, and **C14** have their calculated band gaps of 3.01, 2.55, 2.46, 2.85, 2.46, and 2.53 eV, respectively. Since linear oligothiophenes are planar[25] and cyclic ones are not, the band gap of cyclics is always wider than that in a linear one. The theoretical result obtained in ref 11 predicting the band gap in **C14** to be lower than that in polythiophene itself is an artifact from our point of view produced by approximate determination of the band gap as the HOMO−LUMO energy difference. As a matter of fact, there is a clear correlation between the interring angle of cyclic oligothiophenes and their band gaps, which is even more important than the number of thiophene units

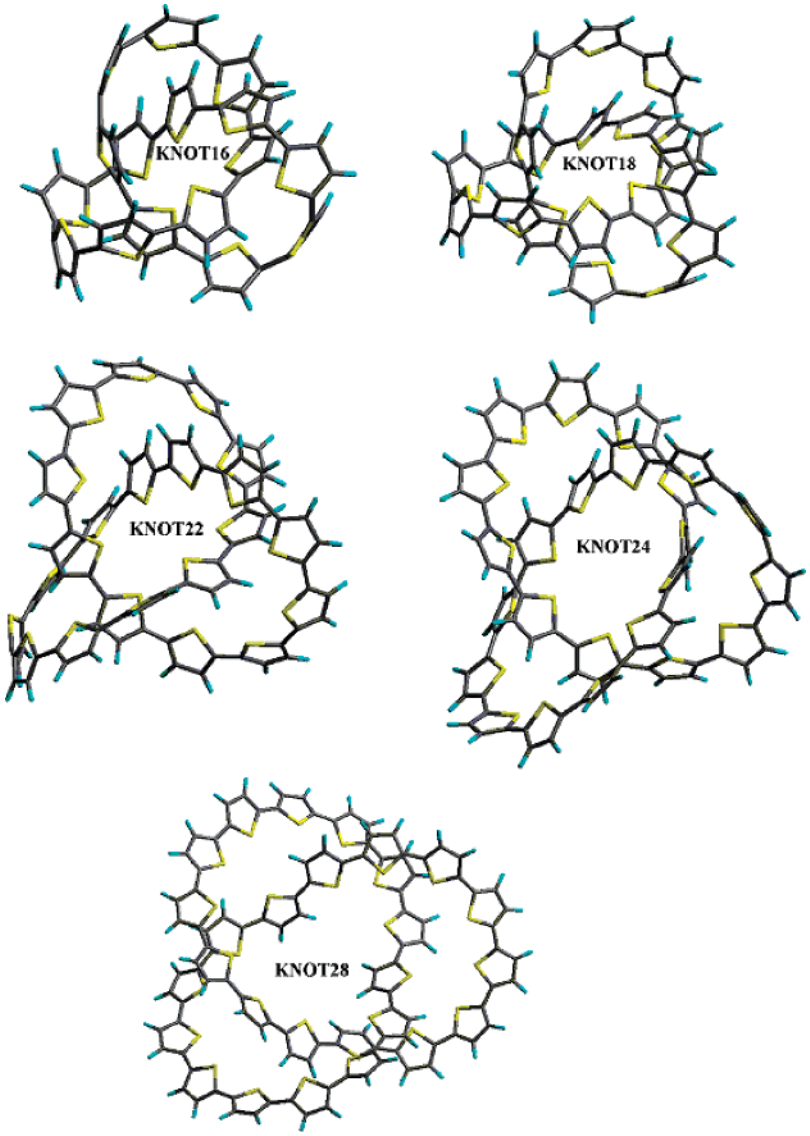

Figure 4. BHandHLYP optimized structures of knots.

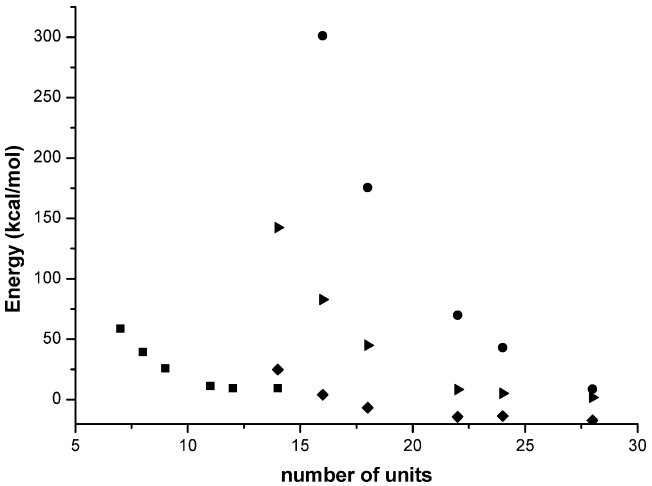

Figure 5. Strain energy in cycles (squares), catenanes (triangles), and knots (circles). Binding energy in catenanes (diamonds).

involved in conjugation. Thus, the inter-ring angle decreases from **C7** to **C11** and increases again for **C14**. The band gap follows this trend (Table 3). In the case of catenanes and knots, there are marked differences. For large catenanes (**CAT18**, **CAT22**, **CAT24**, and **CAT28**), the band gaps are quite similar to those of the corresponding cyclic structures (**C9**, **C11**, **C12**, and **C14**). The band gap of **CAT28** is a bit larger compared to that of **CAT24**. This result evidences that in these catenanes cycles are spectrally independent, behaving as independent chromophores. In **CAT16** and especially **CAT14**, the situation is different. The band gaps in **CAT16** and **CAT14** are smaller than those in corresponding cyclics **C7** and **C8**. The reason for this is that molecular orbitals in these molecules are delocalized over two cycles, increasing electron delocalization (Figure 6). Nevertheless, the band gaps in **CAT14** and **CAT16** are significantly larger compared to those in linear oligothiophene with the same number of thiophene units.

The band gaps in oligothiophene knots are shown in Table 3. Unlike linear oligomers, band gaps increase with the number of thiophene units from **KNOT16** to **KNOT24**, then slightly decrease for **KNOT28**. This unusual behavior is due to very tight geometries of small knots where atomic orbitals overlap not only along the chain but also between thiophene fragments, destroying the one-dimensional nature of the molecule. In **KNOT16** the shortest distances between C and H atoms reach 2.1 Å and between S and H they reach 2.2 Å, which is less than the sum of van der Waals radii of corresponding atoms.

TABLE 2: Bond Lengths (Å) in Thiophene Oligomers Calculated at BHandHLYP/3-21G* Level of Theory

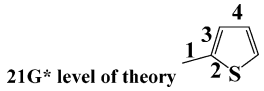

oligomer	1	2	3	4
CAT14	1.460−1.473	1.724−1.753	1.362−1.372	1.427−1.430
CAT16	1.453−1.466	1.723−1.743	1.362−1.370	1.422−1.438
CAT18	1.449−1.455	1.728−1.736	1.365−1.369	1.424−1.428
CAT22	1.444	1.730−1.734	1.365−1.368	1.418−1.421
CAT24	1.443	1.731−1.735	1.365−1.368	1.417
CAT28	1.442−1.445	1.731−1.735	1.365−1.368	1.415
CAT22CR[a]	1.444−1.405	1.725−1.735	1.365−1.397	1.387−1.422
KNOT16	1.471−1.485	1.733−1.785	1.355−1.376	1.414−1.432
KNOT18	1.458−1.481	1.724−1.755	1.363−1.373	1.409−1.430
KNOT22	1.447−1.455	1.725−1.742	1.363−1.371	1.414−1.454
KNOT24	1.447−1.453	1.726−1.740	1.363−1.368	1.414−1.428
KNOT28	1.442−1.450	1.728−1.736	1.364−1.368	1.413−1.422
KNOT22CR[a]	1.404−1.455	1.727−1.742	1.361−1.404	1.381−1.426
C7	1.462−1.472	1.728−1.737	1.361−1.365	1.431−1.434
C8	1.457	1.731	1.366	1.430
C9	1.450	1.732	1.366	1.426
C11	1.444	1.732	1.366	1.420
C11CR[a]	1.415−1.438	1.730−1.735	1.371−1.389	1.395−1.414
C12	1.443	1.733	1.367	1.418
C14	1.443	1.733	1.366	1.415
T28[b]	1.437	1.736	1.368	1.413

[a] Cation radical. [b] Central ring.

TABLE 3: Vertical and Adiabatic Ionization Potentials (IP) Calculated at B97-1/3-21G*//BHandHLYP/3-21G* Level of Theory (eV)[a]

molecule	IP	IP[c]	S0 → S1	E_g
T2	7.59		3.91	4.12; ref 23
T3	6.85	6.2 ± 0.3; ref 21	3.21	3.2; ref 24
T4			3.01	
T6	6.06	5.2 ± 0.3; ref 21	2.55	3.0 ± 0.6; ref 21
T7	5.93		2.46	
T8	5.83		2.40	
T9	5.75		2.35	
T11	5.63, 5.45[b]		2.28	
T12	5.58		2.26	
T14	5.50		2.23	
T16	5.43		2.21	
T18	5.38		2.21	
T22	5.30, 5.16[b]		2.21	
T24	5.27		2.21	
T28	5.21	5.0; ref 22	2.21	2.2; ref 23
C7	6.69		3.08	
C8	6.24		2.85	
C9	6.02		2.66	
C11	5.76, 5.45[b]		2.50	
C12	5.69		2.46	
C14	5.64		2.53	
CAT14	5.99		2.38	
CAT16	5.88		2.71	
CAT18	5.66		2.64	
CAT22	5.47, 5.24[b]		2.54	
CAT24	5.41		2.54	
CAT28	5.39		2.65	
KNOT16	5.92		2.20	
KNOT18	5.87		2.42	
KNOT22	5.54, 5.37[b]		2.49	
KNOT24	5.66		2.78	
KNOT28	5.43		2.62	

[a] S0 → S1 transition energies calculated at ZINDO/S//BHandHLYP/3-21G* level of theory (eV) and experimental band gaps (E_g). [b] Adiabatic ionization potential. [c] Experimental.

For larger knots (**KNOT24** and **KNOT28**), there is no more transversal overlapping of atomic orbitals, and their electronic structure becomes similar to that of cyclic molecules. This is illustrated in Figure 6 where LUMOs of **CAT14**, **CAT28**, **KNOT16**, and **KNOT28** are shown.

Ionization Potentials. The first step in the oxidative doping of the conjugated polymer is the formation of a cation radical (polaron). Cationic species are responsible for hole transport phenomenon by a hopping-type mechanism between adjacent molecules or chains accompanied by geometric relaxation.[26]

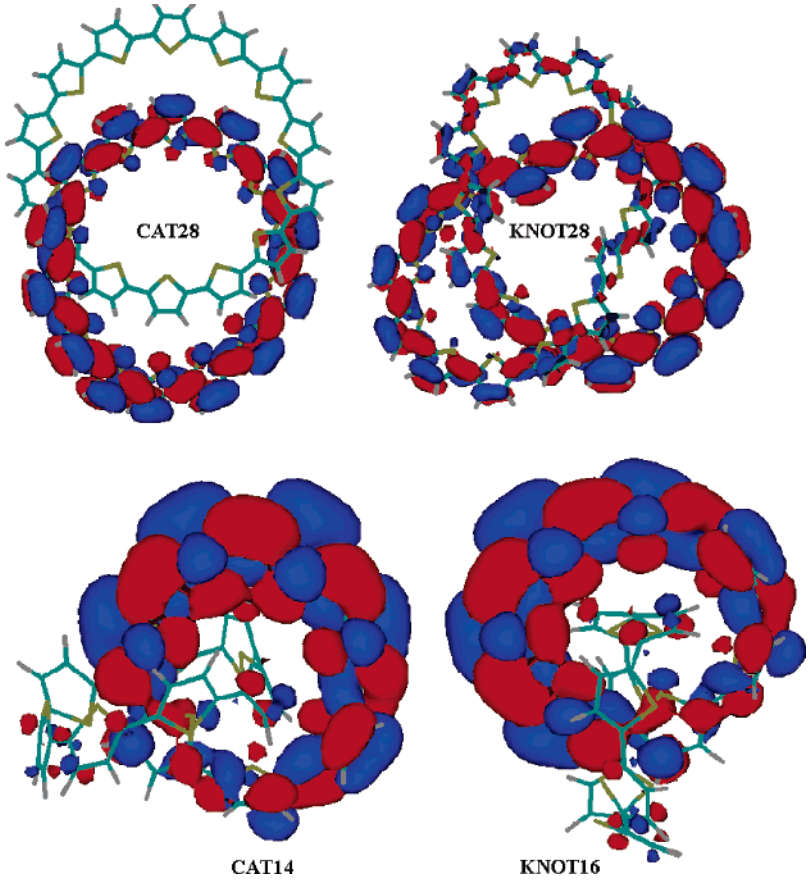

Figure 6. LUMO of **CAT14**, **CAT28**, **KNOT16**, and **KNOT28** calculated at the ZINDO/S//BHandHLYP/3-21G* level.

Table 3 shows vertical and adiabatic ionization potentials (IP) for studied molecules. The difference between vertical and adiabatic IP represents the relaxation energy that is a measure of mobility of a polaron in a conjugated system. Generally, relaxation energies decrease with increasing oligomer chain length as a result of greater positive charge delocalization in a longer oligomer.[27] Vertical IP reflects the conjugation in the neutral molecule and the ability of an electronic system to stabilize positive charge. As seen from Table 3, vertical IPs decrease for catenanes and knots with the number of thiophene units.

Vertical IPs of linear oligomers are lower than those of catenanes, and IPs of catenanes are lower that those of knots with the same number of repeating units. The difference, however, decreases with the number of thiophene fragments, and for **T28**, **CAT28**, and **KNOT28** the difference is only about 0.2 eV. Therefore, knots are the less conjugated systems compared with linear oligomers and catenanes due to increase of inter-ring angle, especially in the case of small knots. Thus, in **KNOT16** inter-ring angles reach 81.4°. Vertical IP correlates with strain energies (Table 3, Figure 5). All other things being equal, higher strain energy corresponds to higher IP for oligomers with the same number of repeating units. For **CAT28** and **KNOT28**, which are almost strain-free, vertical IP is almost the same as that for **T28**.

When comparing vertical IPs of catenanes with those of corresponding cyclic molecules, one can see that for catenanes IPs are always lower compared to those of cyclic molecules, showing that the second ring participates in stabilization of positive charge. The participation of the second ring in stabilization of positive charge can be estimated calculating positive charge distribution in cation radical of a catenane. Thus, calculated positive NPA charges on the second ring in **CAT14**, **CAT16**, **CAT18**, **CAT22**, **CAT24**, and **CAT28** are +0.49, +0.48, +0.50, +0.49, +0.47, and +0.47, showing that additional stabilization is important for all catenanes. Thus, in nonrelaxed cation radicals of catenanes positive charge is distributed almost equally between two cycles.

In the case of linear polythiophene molecules in the condensed phase (which is the relevant one for materials and devices), nearest-neighbor molecules are likely to function in much the same way.

Cation Radicals. To compare the mobility and polaron delocalization in catenanes and knots with those of linear oligothiophene, full geometry optimization of cation radicals for molecules **T11**, **T22**, **C11**, **CAT22**, and **KNOT22** was carried out. Relaxation energies are linearly related to the square root of the chain length of the linear oligomers.[27] For cyclic oligothiophenes,[11] relaxation energies are larger compared to linear oligomers owing to greater geometry change in cyclic cation radicals on ionization. The calculations show that relaxation energy values for **T11**, **T22**, **C11**, **CAT22**, and **KNOT22** are 0.18, 0.14, 0.31, 0.23, and 0.17 eV, respectively. The relaxation energies decrease with the number of repeating units for linear oligomers, and the relaxation energy of **C11** is higher compared to that of **T11** in accordance with ref 11. The relaxation energy of **C11** is higher compared to that of corresponding catenane **CAT22**. This fact can be interpreted in two ways. First, the polaron delocalization is greater in **CAT22**, and second, the steric hindrances limit geometry relaxation in cation radical. Figure 7 shows polaron delocalization in cation radical **CAT22**.

As seen, the spin density is localized on a single cycle, similar to the cation radical of **C11** (Figure 7). Therefore, the polaron

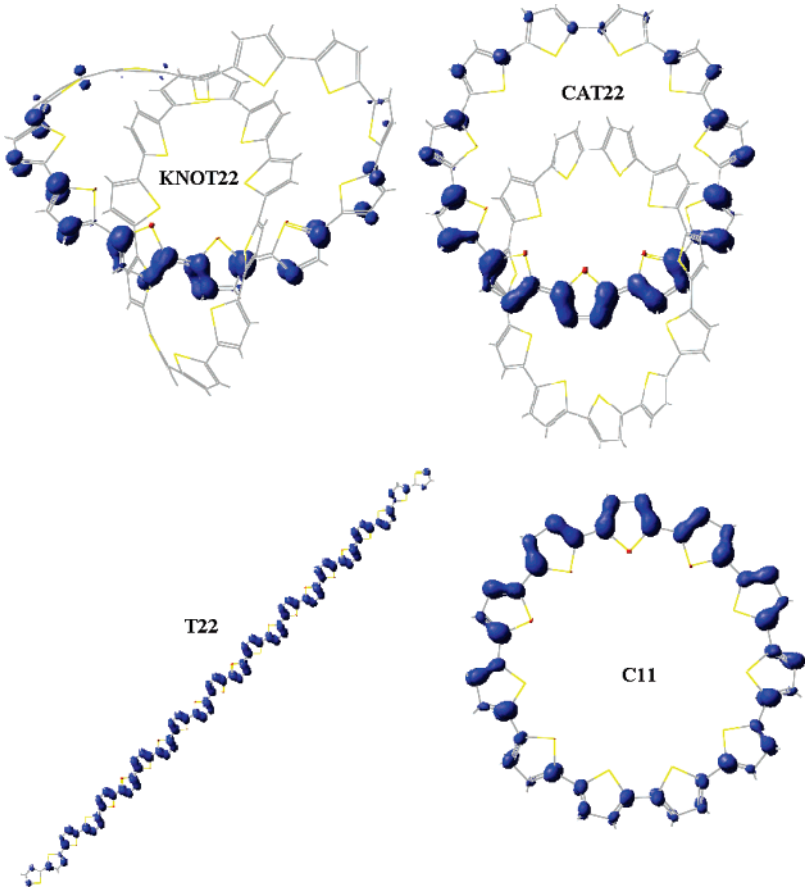

Figure 7. Unpaired spin density in cation radicals of **KNOT22**, **CAT22**, **T22**, and **C11** calculated at the UB97-1/3-21G*//BHandHLYP/3-21G* level of theory.

delocalization is not the reason for lower relaxation energy in **CAT22**. On the other hand, the maximum inter-ring angle in **C11** decreases on ionization from 35.1° to 25.5° while in **CAT22** it decreases from 36.0° to 32.7° due to restricted mobility of thiophene units in oligothiophene cycles in **CAT22**. Nevertheless, adiabatic IP in **CAT22** is a bit lower compared to that of **C11** (Table 3), which can be attributed to the polarization stabilization of positive charge by the second ring. This is illustrated by the increase in binding energy between cyclic oligothiophenes in cation radical **CAT22** compared to neutral molecule from −14.2 to −19.0 kcal/mol. In **KNOT22**, the smaller relaxation energy and higher IP compared to that of **CAT22** is clearly related to steric hindrances; the maximum inter-ring angle even increases on ionization from 52.9° to 54.2°. Therefore, both catenanes and knots have a larger relaxation energy compared to that of their linear analogue, which will make the charge transport energetically more demanding.

In catenanes and especially knots, the polaron is much more localized compared to that of the linear oligomer. The geometry relaxation on ionization results in localization of a polaron. As seen from Figure 7, the polaron localization is the most notorious in **KNOT22** (about 8 to 9 thiophene units), while in **T22** the polaron is delocalized over the whole oligomer chain. In **CAT22**, the polaron is delocalized only over one cycle. Unlike the vertical ionization process where positive charge is distributed almost uniformly over two cycles, adiabatic ionization leads to charge localization with +0.99 charge localized on one cycle. It is important to note that in all cases polaron delocalization is not uniform what is reflected in nonuniform spin density distribution and nonuniform bond lengths. In the area of highest spin density thiophene rings have strong contribution from quinoid structure with very low inter-ring angle, while in the area of low spin density molecular geometry resembles that of neutral molecule. Thus, in **KNOT22** the inter-ring distance and the C3−C4 bond in the area of polaron localization are 1.404 and 1.381 Å, while outside this area they are 1.455 and 1.426 Å, respectively. A similar situation holds for the cation radicals of **C11** and **CAT22**, where polaron is localized mostly on one side of the cycle. Similar asymmetrical distribution of positive charge was calculated for **C12** in the case of bipolaron formation.[28] It is noteworthy that, in cyclic anti conformers, uniform delocalization of a polaron over the cycle was observed.[11]

Conclusions

Oligothiophene catenanes and knots are interesting organic materials. The viable synthetic targets are the catenanes with more than 18 and knots larger than 22 repeating thiophene units. Smaller molecules are excessively strained. A knot with the same number of thiophene units is more strained than a catenane. Small catenanes and knots show strong transversal electronic coupling destroying one-dimensionality of molecules reflecting in smaller band gaps compared to larger ones. IPs of knots and catenanes are always higher compared to those of linear oligomers due to less effective conjugation. The ionization of catenanes and knots causes formation of localized polaron. In the case of **KNOT22**, the polaron is delocalized over 8 to 9 thiophene units, while in **CAT22**, the polaron is localized over only one ring, leaving another intact. It was found that, unlike anti cyclic conformers where the polaron is uniformly delocalized, syn cyclic structures form localized polarons.

Acknowledgment. This research was carried out with the support of Grant IN100806/17 from DGAPA.

Note Added after ASAP Publication. This article was released ASAP on August 1, 2006. The caption for Figure 5 has been revised. The correct version was posted on August 8, 2006.

References and Notes

(1) (a) Li, W. S.; Jiang, D. L.; Aida T. *Angew. Chem., Int. Ed.* **2004**, *43*, 2943. (b) Thomas, T. P.; Patri, A. K.; Myc, A.; Myaing, M. T.; Ye, J. Y.; Norris, T. B.; Baker, J. R., Jr. *Biomacromolecules* **2004**, *5*, 2269. (c) Cravino, A.; Roquet, S.; Leriche, P.; Aleveque, O.; Frere P.; Roncali, J. *Chem. Commun.* **2006**, 1416. (d) Meier, H.; Lehmann, M.; Holst, H. C.; Schwöppe, D. *Tetrahedron* **2004**, *60*, 6881. (e) Toyota, S.; Goichi, M.; Kotani, M. *Angew. Chem., Int. Ed.* **2004**, *43*, 2248. (f) Baxter, P. N. *J. Org. Chem.* **2001**, *66*, 4170.

(2) (a) Prosa, T. J.; Winokur, M. J.; McCullough, R. D. *Macromolecules* **1996**, *29*, 3654. (b) McCullough, R. D. *Adv. Mater.* **1998**, *10*, 93. (c) Chen, T. A.; Wu, X.; Rieke, R. D. *J. Am. Chem. Soc.* **1995**, *117*, 233.

(3) Bao, Z.; Dodabalapur, A.; Lovinger, A. J. *Appl. Phys. Lett.* **1996**, *69*, 4108.

(4) Fichou, D., Ed. *Handbook of Oligo and Polythiophenes*; Wiley-VCH: Weinheim, Germany, 1999.

(5) (a) Horowitz, G.; Peng, X.; Fichou, D.; Garnier, F. *J. Appl. Phys.* **1990**, *67*, 528. (b) Paloheimo, J.; Kuivalainen, P.; Stubb, H.; Vuorimaa, E.; Yli-Lahti, P. *Appl. Phys. Lett.* **1990**, *56*, 1157.

(6) (a) Perepichka, I. F.; Perepichka, D. F.; Meng, H.; Wudl, F. *Adv. Mater.* **2005**, *17*, 2281. (b) Geiger, F.; Stoldt, M.; Schweizer, H.; Baüerle, P.; Umbach, E. *Adv. Mater.* **1993**, *5*, 922.

(7) (a) Brabec, C. J.; Sariciftci, N. S.; Hummelen, J. C. *Adv. Funct. Mater.* **2001**, *11*, 15. (b) Hoppe, H.; Sariciftci, N. S. *J. Mater. Res.* **2004**, *19*, 1924.

(8) (a) Fuhrmann, G.; Debaerdemaeker, T.; Bäuerle, P. *Chem. Commun.* **2003**, 948. (b) Krömer, J.; Rios-Carreras, I.; Fuhrmann, G.; Musch, C.; Wunderlin, M.; Dabaerdemaeker, T.; Mena-Osteritz, E.; Bäuerle, P. *Angew. Chem., Int. Ed.* **2000**, *39*, 3481.

(9) (a) Seidel, D.; Lynch, V.; Sessler, J. L. *Angew. Chem., Int. Ed.* **2002**, *41*, 1422. (b) Köhler, T.; Seidel, D.; Lynch, V.; Arp, F. O.; Ou, Z.; Kadish, K. M.; Sessler, J. L. *J. Am. Chem. Soc.* **2003**, *125*, 6872. (c) Gorski, A.; Koehler, T.; Seidel, D.; Lee, J. T.; Orzanowska, G.; Sessler, J. L.; Waluk, J. *Chem.*−*Eur. J.* **2005**, *11*, 4179.

(10) (a) Bednarz, M.; Rwineker, P.; Mena-Osteritz, E.; Bäuerle, P. *J. Lumin.* **2004**, *110*, 225. (b) Mena-Osteritz, E.; Bäuerle, P. *Adv. Mater.* **2001**, *13*, 243. (c) Mena-Osteritz, E. *Adv. Mater.* **2002**, *14*, 609. (d) Casado, J.; Hernández, V.; Ponce Ortiz, R.; Ruiz Delgado, M. C.; López Navarrete, J. T.; Fuhrmann, G.; Bäuerle, P. *J. Raman Spectrosc.* **2004**, *35*, 592.

(11) Sanjio, S. Z.; Bendikov, M. *J. Org. Chem.* **2006**, *71*, 2972.

(12) (a) Frisch, H. L.; Wasserman, E. *J. Am. Chem. Soc.* **1961**, *83*, 3789. (b) Chambron, J.-C.; Dietrich-Buchecker, C.; Sauvage, J.-P. *Top. Curr. Chem.* **1993**, *165*, 132.

(13) (a) Lukin, O.; Vögtle, F. *Angew. Chem., Int. Ed.* **2005**, *44*, 1456. (b) Raymo, F. M.; Stoddart, J. F. *Chem. Rev.* **1999**, *99*, 1643.

(14) Horowitz, G.; Bachet, B.; Yassar, A.; Lang, P.; Demanze, F.; Fave, J.-L.; Garnier, F. *Chem. Mater.* **1996**, *7*, 1337.

(15) Ridley, J. E.; Zerner, M. C. *Theor. Chim. Acta* **1973**, *32*, 111.

(16) (a) Silva López, C.; Nieto Faza, O.; López Estevez, S.; de Lera, A. R. *J. Comput. Chem.* **2006**, *27*, 116. (b) Khan, M. S.; Khan, Z. H. *Spectrochim. Acta, Part A* **2003**, *59*, 1409. (c) Hutchison, G. R.; Ratner, M. A.; Marks, T. J. *J. Phys. Chem. A* **2002**, *106*, 10596.

(17) Hamprecht, F. A.; Cohen, A. J.; Tozer, D. J.; Handy, N. C. *J. Chem. Phys.* **1998**, *109*, 6264.

(18) Frisch, M. J.; Trucks, G. W.; Schlegel, H. B.; Scuseria, G. E.; Robb, M. A.; Cheeseman, J. R.; Montgomery, J. A., Jr.; Vreven, T.; Kudin, K. N.; Burant, J. C.; Millam, J. M.; Iyengar, S. S.; Tomasi, J.; Barone, V.; Mennucci, B.; Cossi, M.; Scalmani, G.; Rega, N.; Petersson, G. A.; Nakatsuji, H.; Hada, M.; Ehara, M.; Toyota, K.; Fukuda, R.; Hasegawa, J.; Ishida, M.; Nakajima, T.; Honda, Y.; Kitao, O.; Nakai, H.; Klene, M.; Li, X.; Knox, J. E.; Hratchian, H. P.; Cross, J. B.; Bakken, V.; Adamo, C.; Jaramillo, J.; Gomperts, R.; Stratmann, R. E.; Yazyev, O.; Austin, A. J.; Cammi, R.; Pomelli, C.; Ochterski, J. W.; Ayala, P. Y.; Morokuma, K.; Voth, G. A.; Salvador, P.; Dannenberg, J. J.; Zakrzewski, V. G.; Dapprich, S.; Daniels, A. D.; Strain, M. C.; Farkas, O.; Malick, D. K.; Rabuck, A. D.; Raghavachari, K.; Foresman, J. B.; Ortiz, J. V.; Cui, Q.; Baboul, A. G.; Clifford, S.; Cioslowski, J.; Stefanov, B. B.; Liu, G.; Liashenko, A.; Piskorz, P.; Komaromi, I.; Martin, R. L.; Fox, D. J.; Keith, T.; Al-Laham, M. A.; Peng, C. Y.; Nanayakkara, A.; Challacombe, M.; Gill, P. M. W.; Johnson, B.; Chen, W.; Wong, M. W.; Gonzalez, C.; Pople, J. A. *Gaussian 03*, revision B.04; Gaussian, Inc.: Pittsburgh, PA, 2003.

(19) Krömer, J.; Carreras, I R.; Fuhrmann, G.; Musch, K.; Wunderlin, M.; Debaerdemaeker, T.; Mena Osteritz, E.; Bäuerle, M. *Angew. Chem., Int. Ed.* **2000**, *39*, 3481.

(20) Greenberg, A.; Liebman, J. F. *Strained Organic Molecules*; Academic Press: New York, 1978; p 94.

(21) Tepavcevic, S.; Wroble, A. T.; Bissen, M.; Wallace, D. J.; Choi, Y.; Hanley, L. *J. Phys. Chem. B* **2005**, *109*, 7134.

(22) Salzner, U.; Pickup, P.; Poirier, R.; Lagowski, J. *J. Phys. Chem. A* **1998**, *102*, 2572.

(23) Brédas, J. L.; Silbey, R.; Boudreaux, D. S.; Chance, R. R. *J. Am. Chem. Soc.* **1983**, *105*, 6555.

(24) Choi, Y.; Tepavcevic, S.; Xu, Z.; Hanley, L. *Chem. Mater.* **2004**, *16*, 1924.

(25) Bäuerle, P. Oligothiophenes. In *Electronic Materials: The Oligomer Approach*; Müllen, K., Wegner, G., Eds.; Wiley-VCH: Weinheim, Germany, 1998.

(26) (a) Brédas, J. L.; Calbert, J. P.; da Silva, D. A.; Cornil, J. *Proc. Natl. Acad. Sci. U.S.A.* **2002**, *99*, 5804. (b) Cornil, J.; Beljonne, D.; Calbert, J. P.; Brédas, J. L. *Adv. Mater.* **2001**, *13*, 1053.

(27) Hutchison, G. R.; Ratner, M. A.; Marks, T. J. *J. Am. Chem. Soc.* **2005**, *127*, 2339.

(28) Tol, A. J. W. *Synth. Met.* **1995**, *74*, 95.